ACS APPLIED MATERIALS & INTERFACES

RESEARCH ARTICLE

www.acsami.org

Improving Nanoparticle Dispersion and Charge Transfer in Cadmium Telluride Tetrapod and Conjugated Polymer Blends

Todd C. Monson,[*,†] Christopher W. Hollars,[‡,§] Christine A. Orme,[⊥] and Thomas Huser[§,#]

[†]Sandia National Laboratories, Nanomaterials Sciences, P.O. Box 5800, MS 1415, Albuquerque, New Mexico 87185-1415, United States

[‡]MRIGlobal, 425 Volker Boulevard, Kansas City, Missouri 64110, United States

[§]NSF Center for Biophotonics Science and Technology, University of California, Davis, 2700 Stockton Boulevard, Suite 1400, Sacramento, California 95817, United States

[⊥]Physical and Life Sciences Directorate, Lawrence Livermore National Laboratory, M/S L-367, 7000 East Avenue, Livermore, California 94551, United States

[#]Department of Internal Medicine, University of California, Davis, Sacramento, California 95817, United States

Supporting Information

ABSTRACT: The dispersion of CdTe tetrapods in a conducting polymer and the resulting charge transfer is studied using a combination of confocal fluorescence microscopy and atomic force microscopy (AFM). The results of this work show that both the tetrapod dispersion and charge transfer between the CdTe and conducting polymer (P3HT) are greatly enhanced by exchanging the ligands on the surface of the CdTe and by choosing proper solvent mixtures. The ability to experimentally probe the relationship between particle dispersion and charge transfer through the combination of AFM and fluorescence microscopy provides another avenue to assess the performance of polymer/semiconductor nanoparticle composites.

KEYWORDS: conjugated polymers, polymer composites, semiconductor nanoparticles, confocal fluorescence microscope, AFM, fluoresence

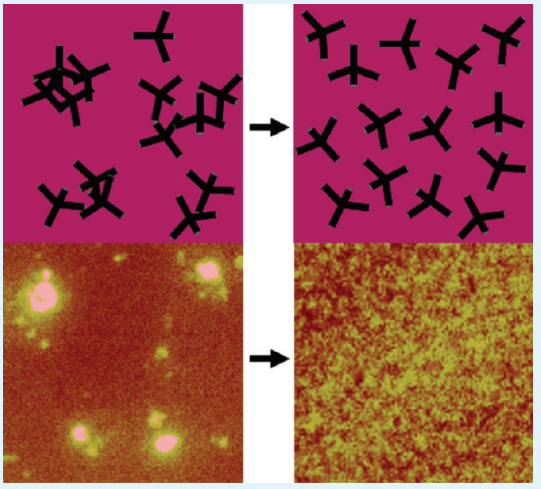

INTRODUCTION

Polymers have tremendous potential to make an impact in many types of flexible electronic and optical devices.[1−4] Organic based devices are relatively cheap and easy to manufacture when compared to traditional inorganic devices, as they avoid high temperature processing and complex lithography. Polymer based devices are also amenable to mass production using inkjet technologies.[5,6] When a polymer cannot be chosen or engineered with the exact properties desired, it is often practical to incorporate inorganic nanoparticles into the polymer matrix and improve the final composite's properties (optical absorption, charge mobility, dielectric constant, etc.). The benefits of nanoparticle/polymer composites has been shown in a variety of different applications including photorefractives, solar cells, dielectric materials, and organic light-emitting diodes (OLEDs).[7−14]

Through careful control of their synthesis, the diameter of nanospheres and nanorods can be controlled, which in turn affects their electronic and optical properties, i.e. the nanoparticle bandgap. By properly choosing the material and size of nanoparticles added to a polymer matrix, the properties of the resulting composite can be tuned to match the desired application. One specific example of an application where a nanoparticle/polymer composite is useful is in addressing the fact that the typical exciton diffusion length in organic photovoltaics (OPVs) is only approximately 10 nm.[15−17] Blending nanoparticles into a hole-conducting polymer for photovoltaic applications provides sites for exciton charge separation prior to recombination, similar to bulk heterojunction fullerene/conducting polymer solar cells.

Although great strides have been made in the synthesis of semiconductor nanoparticles, allowing us to control their size, shape, aspect ratios, composition, and surface chemistry,[18−22] the full potential of improving organic device performance through polymer/nanoparticle blends has not yet been fully realized. Much of the challenge lies in choosing the proper ligands to passivate the semiconductor surface and at the same time allow control over the blending and dispersion of the nanoparticles within a polymer matrix.[23,24] In addition, controlling the nanoparticle surfactant can have a great effect on the charge transfer between

Received: December 10, 2010
Accepted: March 15, 2011
Published: March 15, 2011

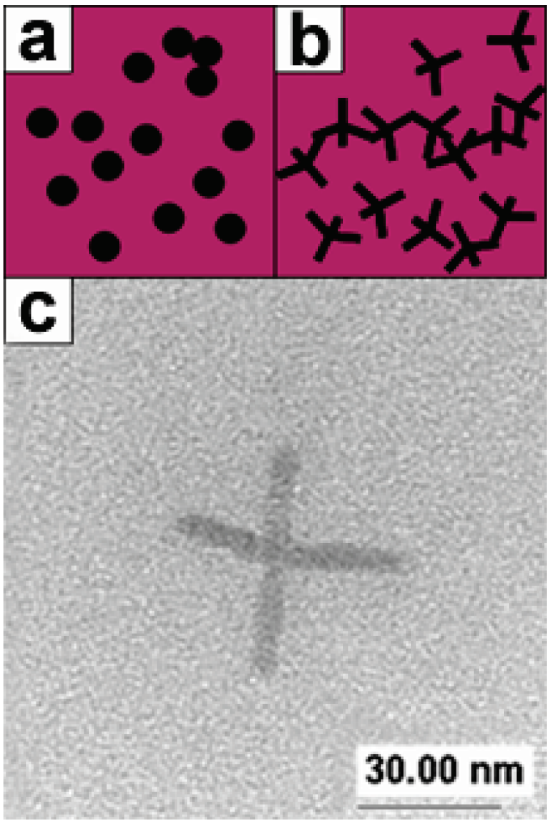

Figure 1. (a) Illustration of a polymer film blended with particles or particle agglomerates. A pathway for electron transport is not present. (b) Illustration of a polymer film blended with tetrapods of sufficient density to form a pathway for electron transport. (c) TEM image of a sample CdTe tetrapod used in this study.

the polymer matrix and the nanoparticles, providing a pathway to potentially tailor this interaction.

We set out to blend the hole-conducting polymer regioregular poly(3-hexylthiophene) (RR P3HT), with CdTe tetrapods and examine the spatiotemporal charge transfer between the inorganic semiconductor and polymer. There are a number of potential applications for such a composite of semiconducting nanoparticles and conducting polymer such as OPVs and photorefractive devices. RR P3HT was chosen because it has one of the highest reported hole mobilities of conjugated polymers (as high as 0.1 $cm^2 V^{-1} s^{-1}$), which can vary depending on the molecular weight of the polymer and the ordering of the film.[25−31] We focused on the tetrapod geometry of CdTe since the rod structure could potentially provide a much better pathway for electron transport than nanospheres.[23] Tetrapods will also be much less sensitive to orientation than nanorods within a polymer matrix. One can imagine if CdTe tetrapods were used in a device such as a solar cell that at the proper blend mix, they can readily form a network of overlapping rod portions. The tetrapods can then form a pathway for electrons along their axes from one electrode to another, no matter how random their orientation within the polymer matrix. The same cannot be said for semiconductor nanorods. In fact, nanorods have a tendency to align themselves parallel to the electrode surfaces, when using typical processing techniques such as spin or dip coating, rather than form a pathway for electrons from one electrode to another.[32] An illustration of the benefit of blending tetrapods in a polymer matrix versus any other particle shape can be seen in Figure 1a, b.

Once assembled, our films were analyzed using a combined atomic force microscope (AFM) and confocal fluorescence microscope. A confocal fluorescence microscope holding an AFM tip within the confocal probe volume and permitting sample scanning with a piezo scan stage allowed us to simultaneously capture AFM and fluorescence microscope images from the same location in the sample. This technique proved to be a valuable way to analyze polymer/semiconductor nanoparticle blend films. In this way, both topography and charge transfer and quenching information can be obtained and correlated. We believe this technique will prove to be quite valuable in the further investigation of polymer and nanoparticle blend films.

Our data show that adding tri-n-octylphosphine oxide (TOPO) capped CdTe tetrapods to a conducting polymer matrix produced very irregular films. Instead of dispersing evenly throughout the polymer film, the tetrapods agglomerated into large masses. Additionally, the TOPO surfactant hinders charge transfer between the polymer and semiconductor nanoparticles, leading to large areas of fluorescence. Replacing TOPO on the CdTe tetrapods by pyridine lead to the formation of very homogeneous films. Additionally, the well-dispersed CdTe tetrapods exhibited very little fluorescence, indicating that charge transfer between the polymer matrix and nanoparticles was occurring.

EXPERIMENTAL SECTION

Trioctylphosphine (TOP, 90%) was purchased from Fluka and n-Octadecylphosphonic acid (ODPA, 99%) was purchased from Polycarbon Industries. All other chemicals were purchased from Aldrich. No further purification was done before using any of the chemicals.

CdTe tetrapods were synthesized using a TOPO-based synthesis described in detail in the literature at a ratio of Cd:Te of 3:1 and Cd:ODPA (n-octadecylphosphonic acid) of 1:3.[18] These precursor ratios were chosen to yield tetrapods of a rather large aspect ratio while retaining good solubility in organic solvents. The tetrapod arms were approximately 50 nm in length and 5 nm in diameter. A sample transmission electron micrograph (TEM) image of one of these tetrapods is shown in Figure 1c. Additionally, the UV−vis absorption spectra of the CdTe tetrapods is available in Figure S1 in the Supporting Information.

Ligand exchange on the CdTe particles was accomplished by refluxing them in pyridine for a period of eight hours, precipitation of the particles by the addition of excess hexanes, centrifuging, and recovering the particles.[19,23,24,33] This process was repeated three times and is reported to replace more than 95% of the TOPO capping agent on the CdTe surface with pyridine.

To fabricate the sample films, we dissolved regioregular P3HT (MW ≈ 87 000) in either chloroform or a 6.3 vol % pyridine in chloroform mixture along with the measured percentage of CdTe tetrapods. The films were spin-cast using a Chemat Technology KW-4B spin coater at 2500 rpm on clean microscope cover slides from polymer solutions of 0.5 wt %. This yielded films with a thickness of 30−50 nm as measured by AFM. The UV−vis absorption spectra of P3HT films (both annealed and unannealed) are available in the Supporting Information (see Figure S2). Photoluminescence (PL) spectra of P3HT are also available in the Supporting Information (see Figure S3).

These films were characterized using a confocal fluorescence microscope with the 488 nm line from an argon ion laser (Coherent Innova 70) at 700 μW focused to a diffraction-limited spot. A 100x air objective (0.9 NA) was used on the microscope. All data were collected with the

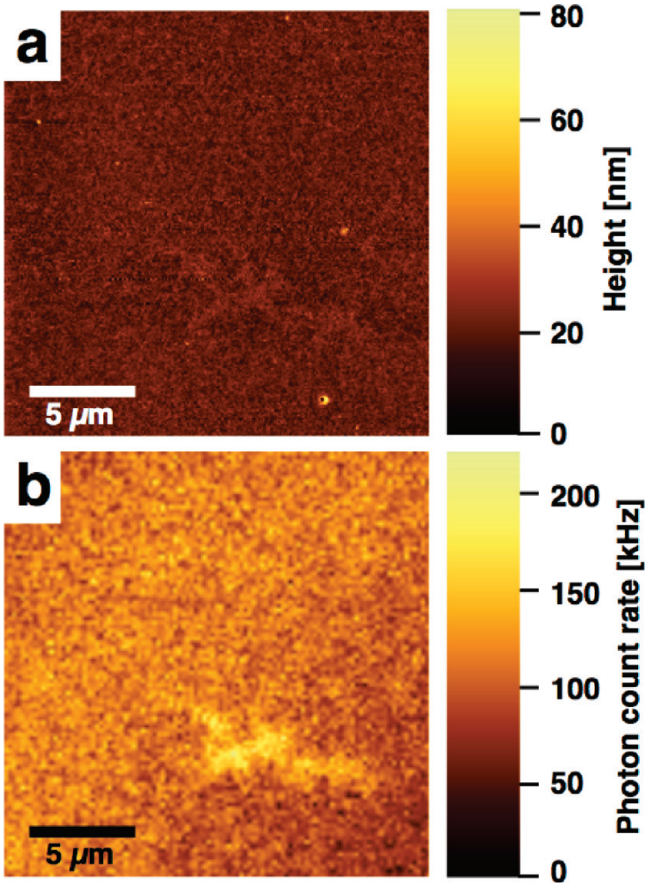

Figure 2. (a) AFM image of a pure RR P3HT polymer film. (b) Corresponding confocal fluorescence microscope image of the same area.

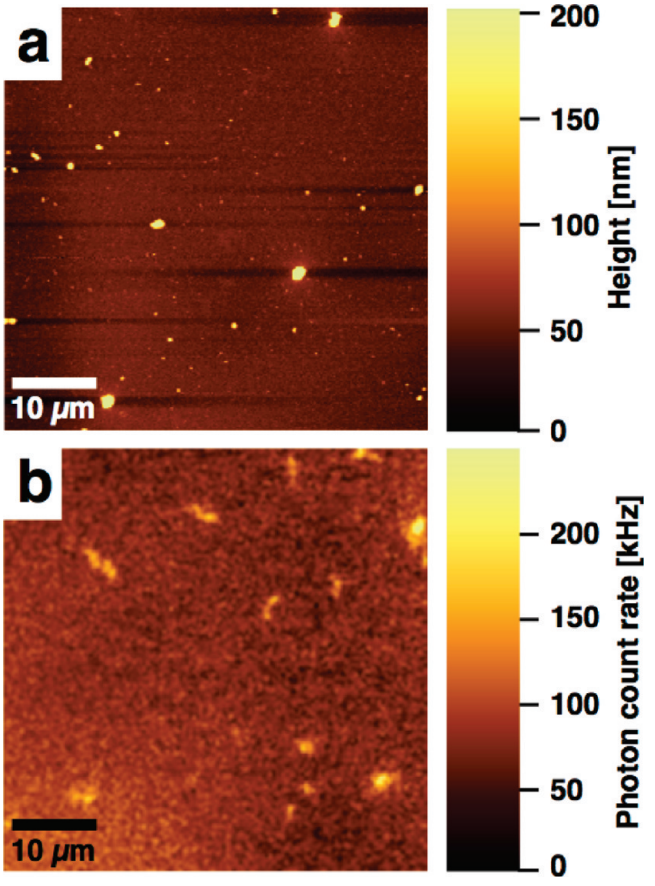

Figure 3. (a) Contact mode AFM image of a 1 wt % CdTe tetrapod concentration in a RR P3HT polymer film. (b) Corresponding confocal fluorescence microscope image of the same area.

same microscope objective, filtered by a 520 nm steep-edge long-pass filter (520LP, Chroma Technology), and detected by red-enhanced single photon counting avalanche photodiode detectors (SPCM-AQR-14, Perkin-Elmer). A Digital Instruments AFM was colocated with the confocal microscope and used to obtain matching AFM images in contact mode.

Fluorescence lifetime imaging data were collected on a commercial FLIM microscope (MicroTime200, Picoquant GmbH, Berlin, Germany). The same detectors and filters as utilized for PL imaging were used, but fluorescence was now excited with a 470 nm picosecond-pulsed diode laser (70 ps pulse duration). Fluorescence was collected with the same APD detectors as mentioned above with 300 ps timing jitter.

RESULTS AND DISCUSSION

Films of P3HT and P3HT/CdTe blends were first prepared with as-synthesized TOPO-capped CdTe tetrapods using chloroform as a solvent. Once both the polymer and tetrapods were dissolved, the blend was spin-cast onto glass cover slides. The CdTe concentrations used were 0, 1, and 10 wt %. Overlapping AFM and confocal fluorescence microscope images were acquired of each of these films. Spin-casting plain P3HT using chloroform as a solvent yielded relatively uniform films containing only a few minor defects as can be seen from Figure 2. When the CdTe tetrapod concentration was increased to just 1 wt % the defects became readily apparent in both the fluorescence microscopy and AFM images (Figure 3). At 10 wt % concentration of tetrapods, the entire film was covered with extremely large nonuniformities, which are readily visible by AFM. These nonuniformities were also the sites of strongly localized fluorescence. Figure 4 provides an excellent example of how these defects visible in the AFM topographic image exhibit perfect overlap with sites where quenching was absent and strong fluorescence is very apparent.

The figures described above demonstrate that even low concentrations of TOPO-coated CdTe particles produced films with significant surface roughness on the order of hundreds of nanometers and a large number of defects in the otherwise smooth film. Overlapping AFM and confocal fluorescence microscope images revealed that areas of nonuniformity in the films also act as sources of high fluorescence. In this case the TOPO-coated tetrapods tend to agglomerate rather than evenly disperse throughout the polymer—solvent mixture and act as defect sites in the films. In addition to hindering the preparation of uniform films, the large nonconducting TOPO molecules appear to also hinder charge transfer between the P3HT and the tetrapods. TOPO prevents the charge separation of excitons formed in the CdTe or in the polymer near the CdTe, causing them to recombine and fluoresce. Without this TOPO barrier, CdTe should act as an electron acceptor and P3HT as a hole acceptor, allowing for charge separation and preventing exciton recombination (see Figure S4 in the Supporting Information). Without a pathway for charge transfer, the tetrapods and their aggregates emit their excitation energy in the form of fluorescence.

To improve the films produced with TOPO-capped CdTe, we sought to replace the TOPO with a significantly smaller ligand that could promote charge transfer. Based on results from the literature,

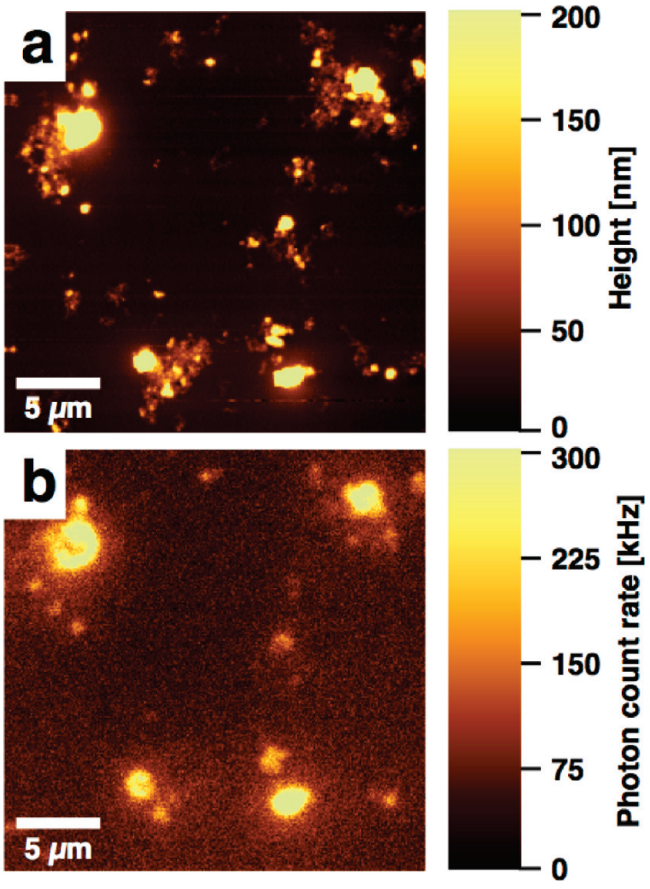

Figure 4. (a) Contact mode AFM image of a 10 wt % CdTe tetrapod concentration in a RR P3HT polymer film. (b) Corresponding confocal fluorescence microscope image of the same area.

pyridine was chosen as the new surfactant because of its small size (relative to TOPO) and conjugated ring structure.[23,24] By also switching to a solvent blend of chloroform and free pyridine it was possible to create homogeneous films where the tetrapods appeared to be evenly dispersed throughout the polymer matrix. Additionally, the pyridine remaining on the surface of the CdTe after spin-casting the films could be removed by annealing the films in a vacuum oven at 120 °C for 4 h.[24] The removal of pyridine allows for better charge transfer between the nanoparticles and the conducting polymer.

Following this logic, films were produced using CdTe tetrapods where the TOPO ligands had been exchanged with pyridine using established procedures.[19,23,24,33] Once pyridine-capped CdTe particles were obtained they were added to the polymer and solvent blend of pyridine and chloroform. By estimating the surface to volume ratio of our tetrapods and following results in the literature a solvent mixture of 6.3 vol % pyridine in chloroform was chosen in order to provide for the most uniform blending of our particles throughout the polymer.[24] These blends were then spin-cast and analyzed using AFM and confocal fluorescence microscopy. Films with CdTe concentrations of 0, 1, 10, and 20 wt % were produced.

All samples were then annealed for 4 h at 120 °C in a vacuum oven to remove the pyridine from the surface of the CdTe particles.[24] Care must be taken when annealing these films in the absence of light and oxygen which can cause photobleaching of the P3HT. When heated in the presence of light or oxygen, the films have a tendency to lighten in color due to a shift in their absorption spectrum. If heated for only a short time under such unfavorable conditions, the photobleaching was found to be reversible. However, if the films were exposed to these conditions for an extended time, the inactivation of the films became permanent.

As expected, the films created using the pyridine-capped CdTe tetrapods showed a dramatic improvement over films with TOPO-capped CdTe particles. The surface roughness of these films decreased dramatically and we were unable to find fluorescent "bright spots". This indicates that the CdTe tetrapods were indeed dispersed evenly throughout the film and charge transfer between the CdTe and the P3HT was not inhibited, allowing for quenching of the fluorescence.

Films of pure P3HT spin-cast with 6.3 vol.-% pyridine in chloroform blend and then annealed showed no defects in the fluorescence microscope images (Figure 5a). When 10 wt % of CdTe was added to the P3HT, the film remained defect-free, indicating both excellent blending of the tetrapods throughout the polymer film and exclent charge transfer between the two components(Figure 5b). Even the films with 20 wt % tetrapods did not show any appreciable defects or fluorescence irregularities (Figure 5c).

Fluorescence lifetime data with corresponding intensity images are displayed in Figure 6. Here, all samples were annealed for 4 h at 120 °C in a vacuum oven. The intensity images with their corresponding scale bars are shown on the left-hand side of the figure and the corresponding fluorescence lifetime images with their matching scale bars are shown on the right-hand side of the figure. A film with 10 wt % CdTe tetrapods passivated with TOPO ligands is shown in the topmost set of images. The intensity image shows many ring shaped regions of high intensity which we believe are defects resulting from clumps of tetrapods where charge transfer between the P3HT and CdTe is inhibited. The lifetime image is fairly uniform and is dominated by fluorescence lifetimes on the order of 1 ns or less. Because there is little or no charge transfer between the CdTe and polymer, excitons do not separate and recombine quickly. Additionally, the presence of many defects provides sites for rapid recombination. The middle set of images contains data from a film of 10 wt % CdTe tetrapods where the TOPO ligands have been exchanged for pyridine molecules. Here, the fluorescence intensity image is much more uniform than in the film with TOPO covered tetrapods. We believe the bright regions are furthest from any tetrapods and thus are regions of higher recombination and intensity. Interestingly, the fluorescence lifetime image contains a much higher percentage of pixels with lifetimes ranging from 4.5 to 3 ns. In this case, the charges from any generated excitons can separate at the CdTe/polymer interface and remain separated for a much longer time before recombining. Finally, the bottom set of images shows a neat P3HT film and is provided for comparison. The neat film produces very uniform intensity and lifetime data. The average lifetime of neat P3HT is considerably shorter than the film containing pyridine capped films. However, it does have a longer average lifetime than the film containing TOPO coated tetrapods, most likely because the neat P3HT film is free of most defects, which provide sites for rapid recombination.

CONCLUSIONS

We have shown that blends of CdTe tetrapods and hole-conducting RR P3HT form very uniform blends by exchanging the TOPO surfactant on the tetrapods with pyridine and dissolving the polymer and nanoparticles in a pyridine and chloroform solvent blend. When spin-cast, these films are very uniform and

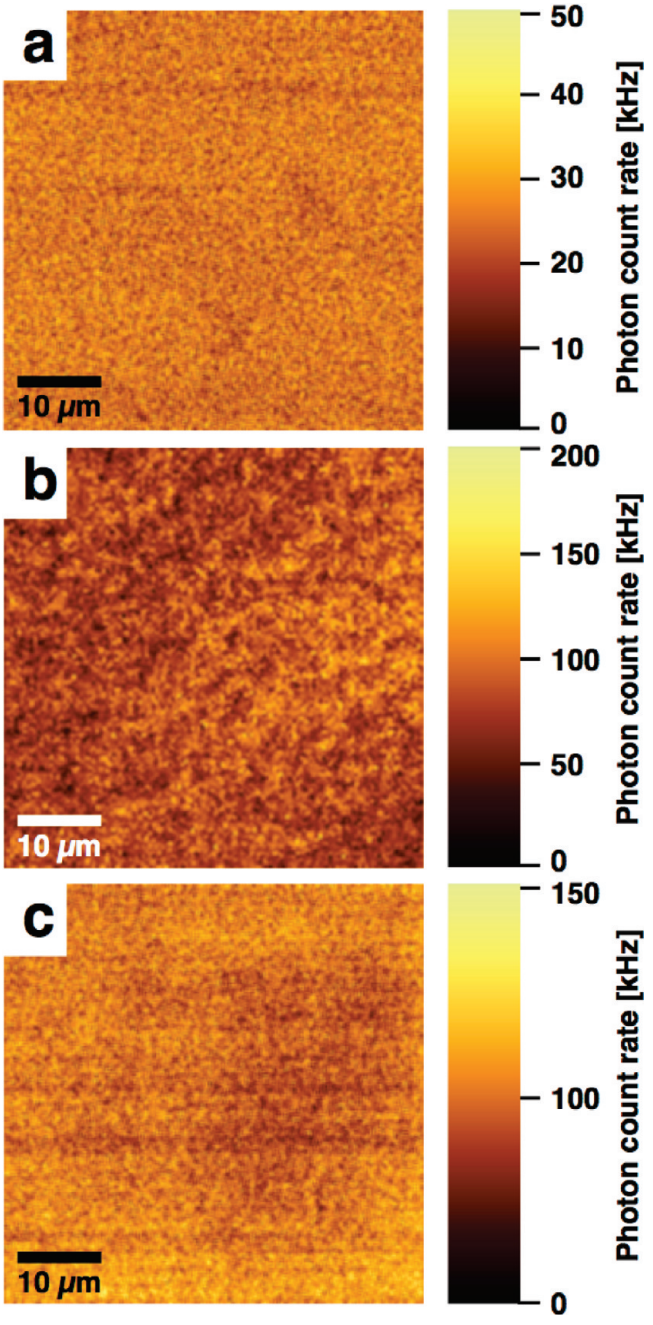

Figure 5. Confocal fluorescence microscope images of (a) pure RR P3HT film, (b) 10 wt % CdTe tetrapod concentration in a RR P3HT polymer film, (c) 20 wt % CdTe tetrapod concentration in a RR P3HT polymer film. All tetrapods were pyridine-capped and the films annealed at 120 °C for 4 h.

exhibit excellent charge transfer throughout the films between semiconductor nanoparticles and organic polymer. Furthermore, we have shown that such films exhibit highly localized defect sites on the micrometer-scale, which can be analyzed by a combined confocal fluorescence microscope/AFM to characterize the spatiotemporal structure of polymer/semiconductor nanocrystal blends for opto-electronic applications.

Future studies should focus on increasing the ratio of CdTe tetrapods in the polymer matrix and continuing to study the effects in these types of films. Measuring the charge mobility in

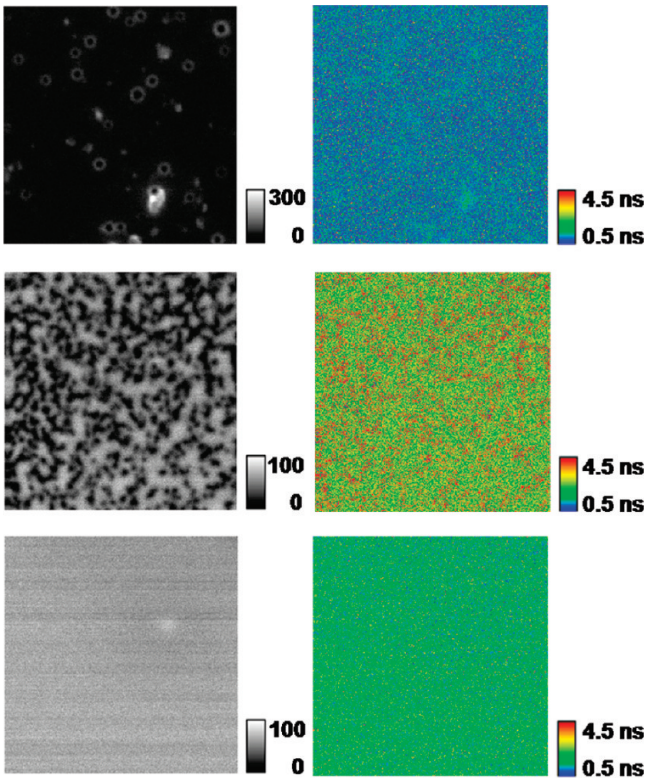

Figure 6. Lifetime data and matching intensity images from a series of CdTe tetrapod and P3HT blend films. The intensity images and their scale bars are on the left and the lifetime images with their corresponding scale bars are on the right. All samples were annealed for 4 h at 120 °C in a vacuum oven. Top: Film of 10 wt % CdTe tetrapods with TOPO ligands. Middle: Film of 10 wt % CdTe tetrapods with pyridine ligands. Bottom: Film of neat P3HT shown for comparison. All images are 20 μm × 20 μm in size. Intensity data are shown as photon counts/pixel with a pixel dwell time of 4 ms.

tetrapod and P3HT blends with an emphasis on finding the percolation density for CdTe tetrapods in RR P3HT will also be an important future step. All of this knowledge could be used to significantly improve the design of polymer/semiconductor nanoparticle blend organic electronic and optical devices.

■ ASSOCIATED CONTENT

Ⓢ Supporting Information. UV−vis absorption spectra of CdTe tetrapods, both annealed and unannealed P3HT films, the PL spectra of P3HT, and the band energy diagram of CdTe and P3HT (PDF). This material is available free of charge via the Internet at http://pubs.acs.org/.

■ AUTHOR INFORMATION

Corresponding Author
*E-mail: tmonson@sandia.gov.

■ ACKNOWLEDGMENT

This work was funded in part by the Air Force Office of Scientific Research. Portions of this work were performed under the auspices of the U.S. Department of Energy by Lawrence Livermore National Laboratory under Contract DE-AC52-07NA27344 as well as Sandia

National Laboratories. Sandia National Laboratories is a multiprogram laboratory operated by Sandia Corporation, a wholly owned subsidiary of Lockheed Martin company, for the U.S. Department of Energy's National Nuclear Security Administration under Contract DE-AC04-94AL85000. T. C. Monson thanks the Lawrence Livermore National Laboratory Military Academic Research Associates (MARA) program for partial support. We thank R. E. Del Sesto and T. J. Boyle for their help in the CdTe tetrapod synthesis.

REFERENCES

(1) Tay, S.; Blanche, P. A.; Voorakaranam, R.; Tunc, A. V.; Lin, W.; Rokutanda, S.; Gu, T.; Flores, D.; Wang, P.; Li, G.; St Hilaire, P.; Thomas, J.; Norwood, R. A.; Yamamoto, M.; Peyghambarian, N. *Nature* **2008**, *451*, 694–698.

(2) Coakley, K. M.; McGehee, M. D. *Chem. Mater.* **2004**, *16*, 4533–4542.

(3) So, F.; Kido, J.; Burrows, P. *MRS Bull.* **2008**, *33*, 663–669.

(4) Dimitrakopoulos, C. D.; Malenfant, P. R. L. *Adv. Mater.* **2002**, *14*, 99–117.

(5) de Gans, B. J.; Duineveld, P. C.; Schubert, U. S. *Adv. Mater.* **2004**, *16*, 203–213.

(6) Sele, C. W.; von Werne, T.; Friend, R. H.; Sirringhaus, H. *Adv. Mater.* **2005**, *17*, 997–1001.

(7) Wei, D.; Baral, J. K.; Osterbacka, R.; Ivaska, A. *J. Mater. Chem.* **2008**, *18*, 1853–1857.

(8) Tomita, Y.; Nakamura, T.; Tago, A. *Opt. Lett.* **2008**, *33*, 1750–1752.

(9) Oey, C. C.; Djurisic, A. B.; Kwong, C. Y.; Cheung, C. H.; Chan, W. K.; Nunzi, J. M.; Chui, P. C. *Thin Solid Films* **2005**, *492*, 253–258.

(10) Fears, T. M.; Anderson, C.; Winiarz, J., G. *J. Chem. Phys.* **2008**, *129*, 154704−1–154704−8.

(11) Schroeder, R.; Majewski, L. A.; Grell, M. *Adv. Mater.* **2005**, *17*, 1535–1539.

(12) Costi, R.; Saunders, A. E.; Elmalem, E.; Salant, A.; Banin, U. *Nano Lett.* **2008**, *8*, 637–641.

(13) Gupta, S.; Zhang, Q. L.; Emrick, T.; Russell, T. P. *Nano Lett.* **2006**, *6*, 2066–2069.

(14) McClure, S. A.; Worfolk, B. J.; Rider, D. A.; Tucker, R. T.; Fordyce, J. A. M.; Fleischauer, M. D.; Harris, K. D.; Brett, M. J.; Buriak, J. M. *ACS Appl. Mater. Interfaces* **2010**, *2*, 219–229.

(15) Coakley, K. M.; McGehee, M. D. *Appl. Phys. Lett.* **2003**, *83*, 3380–3382.

(16) Savenije, T. J.; Warman, J. M.; Goossens, A. *Chem. Phys. Lett.* **1998**, *287*, 148–153.

(17) Pettersson, L. A. A.; Roman, L. S.; Inganas, O. *J. Appl. Phys.* **1999**, *86*, 487–496.

(18) Manna, L.; Milliron, D. J.; Meisel, A.; Scher, E. C.; Alivisatos, A. P. *Nat. Mater.* **2003**, *2*, 382–385.

(19) Kuno, M.; Lee, J. K.; Dabbousi, B. O.; Mikulec, F. V.; Bawendi, M. G. *J. Chem. Phys.* **1997**, *106*, 9869–9882.

(20) Mokari, T.; Rothenberg, E.; Popov, I.; Costi, R.; Banin, U. *Science* **2004**, *304*, 1787–1790.

(21) Li, J. J.; Wang, Y. A.; Guo, W. Z.; Keay, J. C.; Mishima, T. D.; Johnson, M. B.; Peng, X. G. *J. Am. Chem. Soc.* **2003**, *125*, 12567–12575.

(22) Bunge, S. D.; Krueger, K. M.; Boyle, T. J.; Rodriguez, M. A.; Headley, T. J.; Colvin, V. L. *J. Mater. Chem.* **2003**, *13*, 1705–1709.

(23) Huynh, W. U.; Dittmer, J. J.; Alivisatos, A. P. *Science* **2002**, *295*, 2425–2427.

(24) Huynh, W. U.; Dittmer, J. J.; Libby, W. C.; Whiting, G. L.; Alivisatos, A. P. *Adv. Funct. Mater.* **2003**, *13*, 73–79.

(25) Kline, R. J.; McGehee, M. D.; Kadnikova, E. N.; Liu, J. S.; Frechet, J. M. J.; Toney, M. F. *Macromolecules* **2005**, *38*, 3312–3319.

(26) Kline, R. J.; McGehee, M. D.; Kadnikova, E. N.; Liu, J. S.; Frechet, J. M. J. *Adv. Mater.* **2003**, *15*, 1519–1522.

(27) Bao, Z.; Lovinger, A. J.; Dodabalapur, A. *Appl. Phys. Lett.* **1996**, *69*, 3066–3068.

(28) Sirringhaus, H.; Tessler, N.; Friend, R. H. *Science* **1998**, *280*, 1741–1744.

(29) Raja, M.; Lloyd, G. C. R.; Sedghi, N.; Eccleston, W.; Di Lucrezia, R.; Higgins, S. J. *J. Appl. Phys.* **2002**, *92*, 1441–1445.

(30) Sirringhaus, H.; Brown, P. J.; Friend, R. H.; Nielsen, M. M.; Bechgaard, K.; Langeveld-Voss, B. M. W.; Spiering, A. J. H.; Janssen, R. A. J.; Meijer, E. W.; Herwig, P.; de Leeuw, D. M. *Nature* **1999**, *401*, 685–688.

(31) Kobashi, M.; Takeuchi, H. *Macromolecules* **1998**, *31*, 7273–7278.

(32) Sun, B. Q.; Marx, E.; Greenham, N. C. *Nano Lett.* **2003**, *3*, 961–963.

(33) Katari, J. E. B.; Colvin, V. L.; Alivisatos, A. P. *J. Phys. Chem.* **1994**, *98*, 4109–4117.